IOP Publishing Superconductor Science and Technology
Supercond. Sci. Technol. 29 (2016) 084001 (10pp) doi:10.1088/0953-2048/29/8/084001

Trapped field of 1.1 T without flux jumps in an MgB_2 bulk during pulsed field magnetization using a split coil with a soft iron yoke

H Fujishiro[1], H Mochizuki[1], M D Ainslie[2] and T Naito[1]

[1] Department of Materials Science and Engineering, Faculty of Engineering, Iwate University, 4-3-5 Ueda, Morioka 020-8551, Japan
[2] Bulk Superconductivity Group, Department of Engineering, University of Cambridge, Trumpington Street, Cambridge CB2 1PZ, UK

E-mail: fujishiro@iwate-u.ac.jp

Received 14 March 2016, revised 5 May 2016
Accepted for publication 27 May 2016
Published 16 June 2016

Abstract

MgB_2 superconducting bulks have promising potential as trapped field magnets. We have achieved a trapped field of $B_z = 1.1$ T on a high-J_c MgB_2 bulk at 13 K without flux jumps by pulsed field magnetization (PFM) using a split-type coil with a soft iron yoke, which is a record-high trapped field by PFM for bulk MgB_2 to date. The flux jumps, which frequently took place using a solenoid-type coil during PFM, were avoided by using the split-type coil, and the B_z value was enhanced by the insertion of soft iron yoke. The flux dynamics and heat generation/propagation were analyzed during PFM using a numerical simulation, in which the magnetic flux intruded and attenuated slowly in the bulk and tended to align along the axial direction due to the presence of soft iron yoke. The advantages of the split-type coil and the simultaneous use of a soft iron yoke are discussed.

Keywords: pulsed field magnetization, MgB_2 bulk, numerical simulation, flux jump, split-type coil, soft iron yoke

(Some figures may appear in colour only in the online journal)

1. Introduction

MgB_2 superconducting bulks have promising potential as trapped field magnets, such as being rare-earth-free, light-weight and presenting a homogeneous trapped field distribution [1], which are in clear contrast with REBaCuO bulk magnets [2]. The problem of weak-links at grain boundaries can be ignored in MgB_2 polycrystalline bulks due to their long coherence length, ξ, which enable us to realize better and larger polycrystalline bulk magnets below the transition temperature $T_c = 39$ K [3]. Recently, MgB_2 bulks with high critical current density, J_c, have been fabricated by various methods and activated by field-cooled magnetization (FCM) [4–6]. A record-high trapped field of $B_z = 5.4$ T has been attained at 12 K on a single MgB_2 bulk 20 mm in diameter [7].

Pulsed-field magnetization (PFM) has been also investigated to magnetize bulk superconductors, usually using a solenoid-type copper coil and a condenser bank. However, the trapped field, B_z, by PFM is generally lower than that by FCM because of a large temperature rise caused by the dynamic motion of the magnetic flux. Multi-pulse techniques are effective to enhance B_z for REBaCuO bulks due to the reduction of this temperature rise [8, 9]. B_z (PFM) = 5.20 T has been attained on a GdBaCuO bulk 45 mm in diameter at 30 K using a modified multi-pulse technique with stepwise cooling [10], which is a record-high B_z for REBaCuO bulk by PFM to date. The PFM technique has also been applied to MgB_2 bulks [11, 12]. However, B_z (PFM) = 0.81 T at 14 K is the highest value so far for a high-J_c MgB_2 bulk fabricated by the hot isostatic pressing (HIP) method, on which B_z

(FCM) = 2.23 T was trapped at 16 K by FCM [13]. However, flux jumps took place frequently during PFM in the high-J_c MgB_2 bulks and consequently the B_z (PFM) value decreased for higher applied magnetic fields. On the other hand, flux jumps are scarcely observed in low-J_c MgB_2 bulks and even for lower applied fields in high-J_c MgB_2 bulks. The flux dynamics and heat generation in the MgB_2 bulk around 20 K are in clear contrast with those in the REBaCuO bulk at around typical operating temperature of 40 K because of the small specific heat, large thermal conductivity, and a narrow temperature margin against T_c for the MgB_2 bulk. We have previously analyzed and discussed the electromagnetic and thermal instability of a high-J_c MgB_2 bulk using conventional relations, such as the critical thickness, d_c, and the minimum propagation zone length, l_m [14].

Ida *et al* proposed a new PFM technique using a vortex-type coil, which consists of a couple of copper coils [15]. They demonstrated that, using the vortex-type coil at 77 K, the magnetic flux starts to be trapped in the center of the REBaCuO bulk, even for lower pulsed fields, and that the maximum B_z was enhanced in comparison to that obtained using the solenoid-type coil. We have performed the numerical simulation of trapped field, B_z, and temperature, T, after applying a magnetic pulse using the vortex-type coil, and the results of the simulation can reproduce the experimental results well [16]. In this case, the magnetic flux intrudes into the bulk not from the periphery, but mainly from the surface, and the temperature rise during the flux intrusion for the vortex-type coil is smaller than that for the solenoid-type coil. We also performed the PFM experiments for REBaCuO bulks using split-type coil, which is of a similar structure to the vortex-type coil [17, 18]. The trapped field can be enhanced using the split-type coil experimentally, but there are no reports on PFM experiments using the split-type coil for MgB_2 bulks yet. Ikuta *et al* investigated the effect of sandwiching the bulk with a pair of ferromagnetic iron yoke pieces on the trapped field, B_z, and total trapped flux, Φ_z [19]. The magnetic flux distribution became more homogeneous and Φ_z was enhanced by the existence of the yoke, because the magnetic pulse was more effectively applied to the bulk. Gony *et al* reported the effect of iron core during PFM at 77 K using a solenoid-type coil and repeated the insertion and removal of the iron core on the magnetized bulk [20]. The trapped field was enhanced by the existence of the iron core, which comes from the orientation of the flux in the direction of the iron core.

On the basis of our experience with PFM and some indications for the improvement of the PFM technique [15, 19], we expect to avoid flux jumps and enhance the trapped field during PFM for high-J_c MgB_2 bulks using the split-type coil with soft iron yokes. In this study, we investigate the PFM procedure for the high-J_c MgB_2 bulk using a split-type coil and compared this to those for a solenoid-type coil. We also study the effect of the soft iron yoke for the split-type coil to enhance the trapped field, B_z.

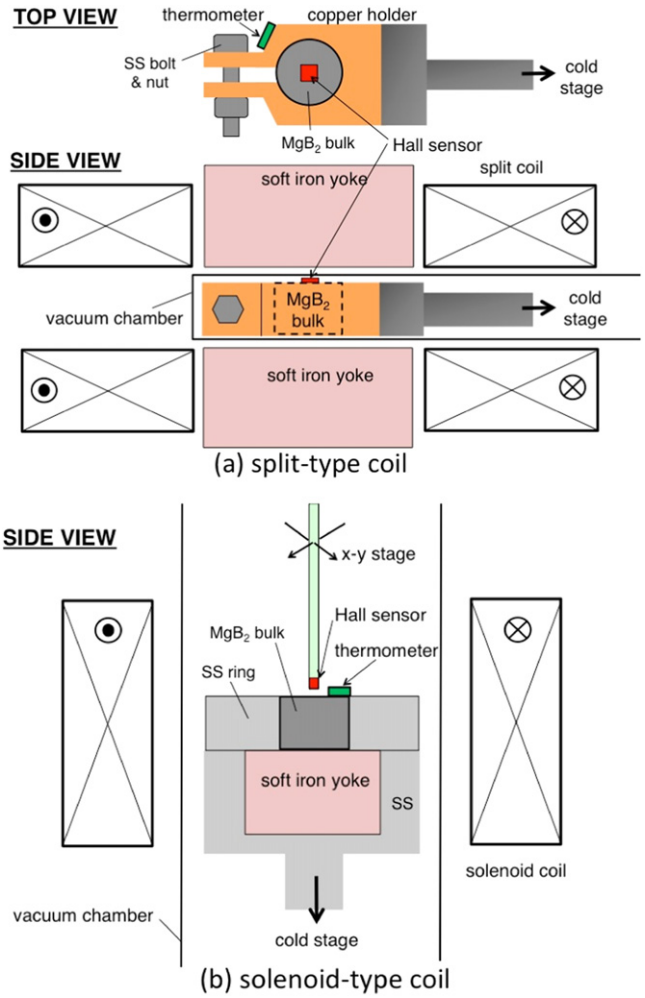

Figure 1. Experimental setup for (a) 'split coil with two yokes' and (b) 'solenoid coil with one yoke'. The PFM experiments were also performed using 'split coil without yoke' in (a).

2. Experimental details

A bulk MgB_2 superconducting disk was fabricated by a HIP method [6]. The diameter and thickness are 22 mm and 15 mm, respectively, and the relative mass density was as high as 93% of the ideal mass density. B_z(FCM) = 2.23 T was achieved at the center of the bulk surface at 16 K by FCM. Figure 1 shows the experimental setup of PFM using the split-type and solenoid-type coils. For the split-type coil shown in figure 1(a), the MgB_2 bulk was fastened in a copper holder with thin indium foil (0.2 mm in thickness) and connected to the cold stage of a Gifford–McMahon cycle, helium refrigerator in the vacuum chamber. A Hall sensor (BHT 921; F W Bell) was adhered to the center of the bulk surface, and the thermometer (Cernox™) was tightly connected to the copper holder. The split-type coil (72 mm inner diameter (ID), 124 mm outer diameter (OD), 35 mm height, wire cross-section of 1.3 × 3.0 mm^2 and 117 turns of each coil), which was submerged in liquid nitrogen, was placed outside the vacuum chamber, in which a pair of soft iron plain, Ni-plated yokes (60 mm in diameter and 65 mm in height) was inserted in the central bores of the coil. This coil setup is named 'split

coil with two yokes'. For comparison, the bulk was magnetized using the split-type coil with the absence of the soft iron yokes, which is named 'split coil without yoke'. The initial temperature, T_s, of the bulk was set to 13 and 20 K, and magnetic pulses, $B_{ex}(t)$, with a peak up to 2.95 T, a rise time of 0.018 s and a duration of 0.18 s were applied via a pulsed current in the coil. The peak of the generated magnetic field is proportional to the flowing current, I; for example, to achieve $B_{ex}(\max) = 1.5$ T at the center of the split coil without any superconductor inserted, $I = 440$ A and 850 A was flown for the 'split coil with two yokes' and 'split coil without yoke', respectively. During PFM, the time evolution of the temperature, $T(t)$, the central field, $B_z(t)$, and the subsequent trapped field, B_z, which was defined as the final value of $B_z(t)$ at 60 s, were measured at the center of the bulk surface. After the removal of the split-type coil 15 min after the pulse application, two-dimensional trapped field profile of B_z was mapped at 2 mm above the bulk surface (on the outer surface of the vacuum chamber) by scanning a Hall sensor (BHA 921; F W Bell) using an x–y stage controller.

In the case of using the solenoid coil, as shown in figure 1(b), the same MgB_2 disk was mounted in a stainless steel (SS) ring (22.1 mm ID, and 56.0 mm OD) using epoxy resin (Stycast 2850™) and was tightly anchored onto the SS holder with a soft iron yoke (40 mm diameter (D) and 20 mm height (H)). This was then connected to the cold stage of a refrigerator using an indium foil [6, 11]. The soft iron yoke is fixed to the magnetizing fixture, so cannot be removed after the PFM is carried out. This coil setup is named 'solenoid coil with one yoke'. The solenoid copper coil (99 mm ID, 121 mm OD, 50 mm H, wire cross-section of 1.3×3.0 mm^2 and 112 turns), which was submerged in liquid nitrogen, was placed outside the vacuum chamber. The initial temperature, T_s, of the bulk was set to 20 K. Magnetic pulses, B_{ex}, up to 2.2 T, with a rise time of 0.013 s and duration of 0.15 s were applied via a pulsed current in the coil. For example, $I = 1040$ A was applied to achieve $B_{ex}(\max) = 1.5$ T at the center of the solenoid coil without any superconductor inserted. The time evolution of the central field, $B_z(t)$, and the subsequent trapped field at 60 s, B_z, at the center of the bulk surface were monitored by a Hall sensor (BHA 921; F W Bell). Two-dimensional trapped field profiles of B_z were mapped in a vacuum chamber 15 min after the pulse application, stepwise with a pitch of 1 mm, by scanning the same Hall sensor using an x–y stage controller. The time evolution of the temperature, $T(t)$, was also measured separately using a thermometer adhered to the bulk surface.

3. Numerical simulation

Based on the experimental setup, three types of models were constructed for the numerical simulation of PFM as shown in figure 2, in which the physical phenomena occurring during the magnetization process are described using the fundamental electromagnetic and thermal equations in axisymmetric coordinates. The details of the numerical simulation have been described elsewhere [14]. The power-n model ($n = 100$) was used to describe the nonlinear E–J characteristic of the MgB_2 bulk. The results of the numerical simulation strongly depend on the $J_c(B, T)$ characteristics of the superconductor [21]. The $J_c(B)$ curve of the MgB_2 bulk at 20 K, which was measured using a small piece cut from a similar bulk by a commercial SQUID magnetometer (MPMS-5T; Quantum Design), was fitted using the following equation

$$J_c(B, T) = \alpha\left\{1 - \left(\frac{T}{T_c}\right)^2\right\}^{\frac{3}{2}} \exp\left[-\left(\frac{B}{B_0}\right)^{\beta}\right], \qquad (1)$$

where $T_c = 39$ K, $\alpha = 4.5 \times 10^9$ A m^{-2}, $B_0 = 1.3$ T and $\beta = 1.7$ are the fitted parameters. When these parameters were used in the simulation for FCM, a trapped field of magnitude at least twice the expected trapped field, was obtained. It was found that the parameter α should be adjusted to a lower value of $\alpha = 5.8 \times 10^8$ A m^{-2} to adequately reproduce the experimental results. This is because the J_c (B, T) value estimated from the magnetization measurement might be overestimated, compared to the real transport J_c (B, T) value, which is in clear contrast to the numerical simulation in MgB_2 bulk for FCM [1].

The applied pulsed field, $B_{ex}(t)$, which is proportional to the current flowing in the coil, was approximated using the following equation with a rise time of $\tau = 0.018$ s for the split coil without yoke and $\tau = 0.013$ s for the solenoid coil without yoke, respectively, which were determined from the experimental results.

$$B_{ex}(t) = B_{ex}\frac{t}{\tau}\exp\left(1 - \frac{t}{\tau}\right). \qquad (2)$$

In the numerical analysis, we set the spacing plate with a thermal conductivity $\kappa_{cont} = 0.5$ W mK^{-1} between the MgB_2 bulk and the metal holder, which artificially represents the cooling power of the refrigerator, the thermal contact conductivity and the thermal conductivity of the inserted indium foil. The temperature dependence of the thermal conductivity, $\kappa(T)$, the specific heat, $C(T)$, and the mass density, d, of the MgB_2 bulk and the SS ring were introduced into the model [14], and these values for the soft iron yoke ($\kappa = 2.4$ W mK^{-1}, $C = 12.7$ J kg^{-1} K^{-1}, $d = 7840$ kg m^{-3}) and copper ($\kappa = 50$ W mK^{-1}, $C = 8.0$ J kg^{-1} K^{-1}, $d = 8960$ kg m^{-3}) are assumed to be temperature independent. The saturation magnetization, $\mu_0 M_{sat}$, the initial relative permeability, $\mu_{r,max}$ ($B < \mu_0 M_{sat}$), and the electrical conductivity, σ, of the soft iron yoke were assumed to be $\mu_0 M_{sat} = 1.6$ T, $\mu_{r,max} = 2000$ and $\sigma = 1.264 \times 10^7$ S m^{-1}, respectively. When the temperature of the bulk exceeds T_c, the electrical conductivity of the region of the bulk is assumed to be 1×10^5 S m^{-1}. Iterative calculations were performed for analyzing the combined problem of electromagnetic fields and heat diffusion using the finite element method implemented in the commercial software package, Photo-Eddy, combined with Photo-Thermo (Photon Ltd, Japan).

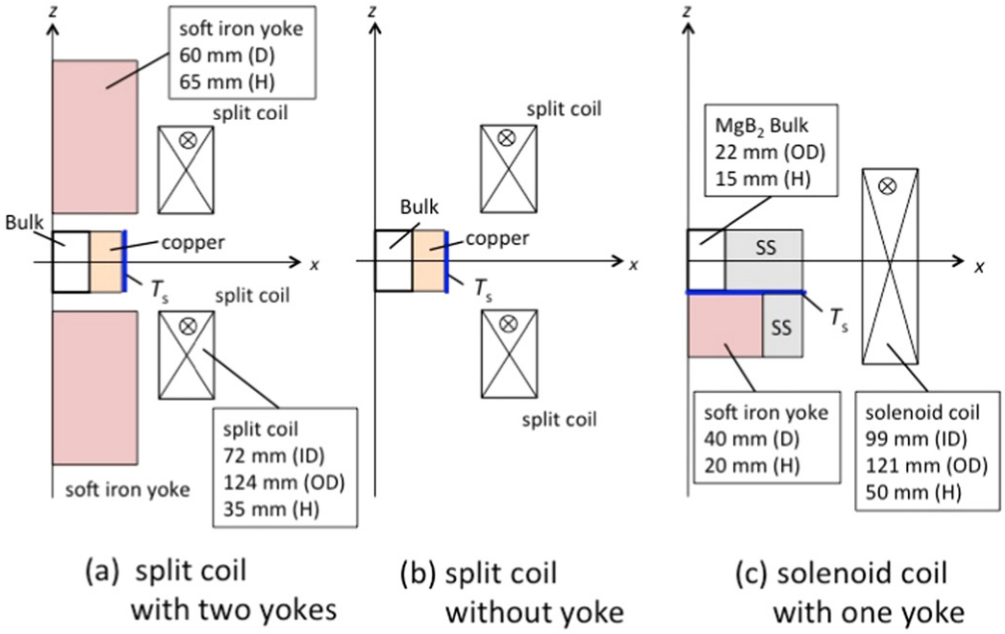

Figure 2. Three types of models for numerical simulation during PFM using (a) split coil with two yokes, (b) split coil without yoke and (c) solenoid coil with one yoke. The dimensions of the MgB_2 bulk, magnetizing coils and the inserted soft iron yokes are also shown.

4. Experimental results

Figure 3(a) presents the trapped field, B_z, on the MgB_2 bulk at $T_s = 20$ K by PFM using the three magnetizing coil cases, as a function of the applied pulsed field, B_{ex}. For the results using the 'solenoid coil with one yoke', which were reported briefly elsewhere [13], the B_z value increases steadily from $B_{ex} = 1.2$ T and attains a maximum value of $B_z = 0.81$ T at $B_{ex} = 2.0$ T. However, a flux jump occurred for a higher field of $B_{ex} = 2.2$ T. In the case of using the 'split coil without yoke', the magnetic flux starts to intrude into the bulk center from $B_{ex} = 0.7$ T, which is lower than that for the solenoid coil, and the B_z value takes a maximum value of $B_z = 0.75$ T at $B_{ex} = 1.3$ T, and then decreases with further increasing B_{ex}. For the case using the 'split coil with two yokes', the maximum trapped field was enhanced to 1.05 T at $B_{ex} = 1.5$ T, and then decreased with increasing B_{ex}. It is important to note that no flux jump occurred, even at higher B_{ex} up to 2.95 T in the case of using the split coil, both with and without the yoke. Figure 3(b) shows B_z at 13 K using the 'split coil with two yokes' as a function of B_{ex}. The trapped field was enhanced with decreasing starting temperature, $T_s = 13$ K; $B_z = 1.10$ T was realized at $B_{ex} = 1.55$ T with no flux jump. The detailed time dependences of the local field, $B_z(t)$, will be discussed later.

The results shown in figure 3(a) were measured under the condition that the soft iron yoke was loaded on the bulk. In this case, the trapped magnetic flux was forced to align along the z-direction due to the existence of yoke. The B_z value after the removal of the split coil with yoke is also shown in figure 3(b). The inset shows the B_z change at 13 K and for $B_{ex} = 1.61$ T. The B_z value decreased from 1.10 to 1.04 T, which results from the absence of the flux alignment effect of the yoke along the z-direction. The similar reduction of B_z by the removal of the yoke was reported in [20].

Figure 4 depicts the time evolution of the applied pulsed field, $B_{ex}(t)$, of 2.2 to 2.3 T in the cases using each pulsed coil, which were measured on the bulk surface at $T_s = 50$ K above T_c. The difference of $B_{ex}(t)$ can be observed for each case, although the profiles for the split coils are quite noisy, which is a result of incomplete electrical shielding of the probe used with the oscilloscope. The time, at which the pulsed magnetic field takes a maximum, was 0.018 s and 0.013 s for the split coil and the solenoid coil, respectively, due to the difference of the coil inductance, L. The presence of the soft iron yoke seems to stop more flux leaving at the bulk position as the pulse reduces during its descending stage. Note that the eddy current may affect the experimental data for heat generation and so on, but we have not considered the influence of the eddy current in the present study.

Figure 5 shows the time evolution of the applied field, $B_{ex}(t)$, and the local field, $B_z(t)$, at the center of the bulk surface using each magnetizing coil. For the case using the solenoid coil at 20 K, shown in figures 5(a) and (b), the magnitude of $B_z(t)$ is smaller than that of $B_{ex}(t)$ with a very slight time delay around the peak of the pulse. After the $B_z(t)$ peak, $B_z(t)$ smoothly decreases and approaches its final value. For $B_{ex} = 2.20$ T, shown in figure 5(b), a flux jump occurred, and a decrease of B_z and the inhomogeneity of the trapped field profile was observed.

On the other hand, for the case using the 'split coil without yoke' at 20 K, shown in figures 5(c) and (d), there is no time delay in $B_z(t)$ at the peak and the peak height of $B_z(t)$ is nearly the same as that of $B_{ex}(t)$. After the peak of the pulse, $B_z(t)$ decreases, then shows an inflection and approaches to its

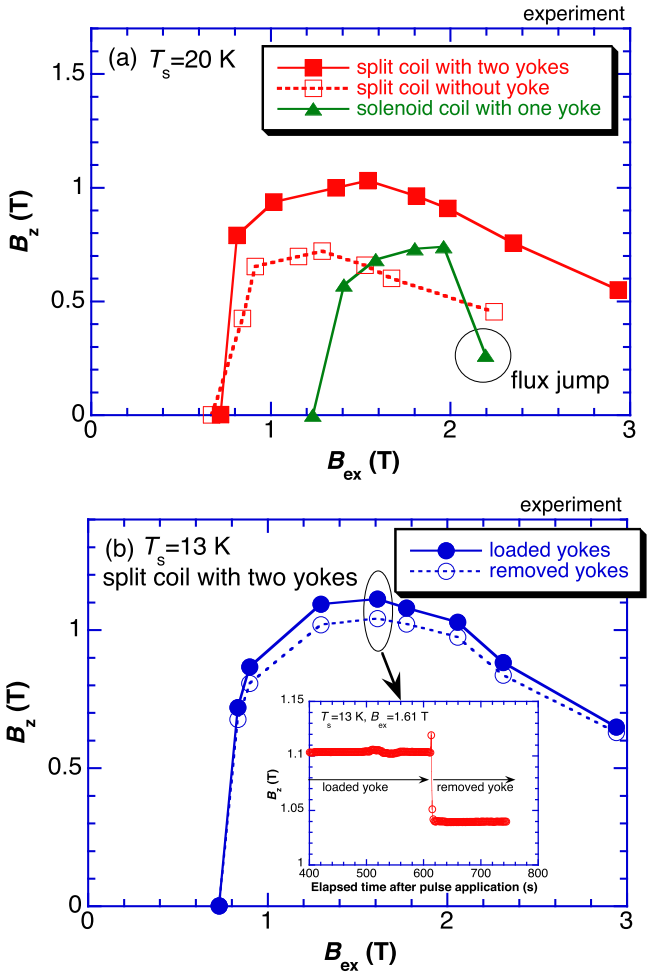

Figure 3. (a) Applied pulsed field, B_{ex}, dependence of the trapped field, B_z, for each case at $T_s = 20$ K: using the split coil with two yokes, split coil without yoke and solenoid coil with one yoke. (b) B_{ex} dependence of B_z before and after the removal of the soft iron yokes at 13 K. The trapped field change for $B_{ex} = 1.61$ T is also shown in the inset.

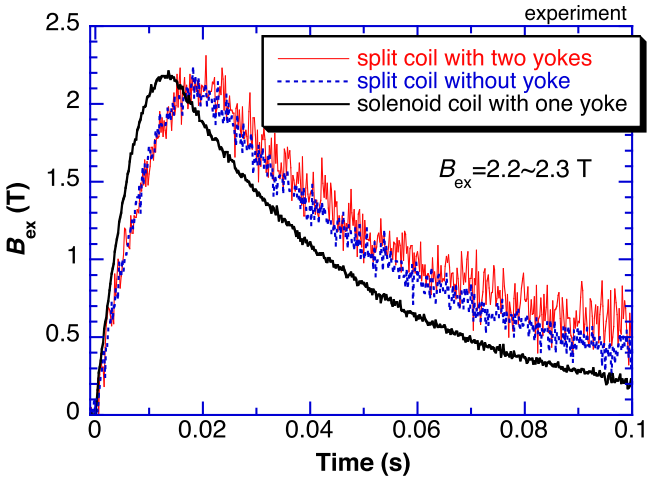

Figure 4. Time evolution of the applied pulsed field, $B_{ex}(t)$, for 'split coil with two yokes', 'split coil without yoke' and 'solenoid coil with one yoke'.

final value, which is in clear contrast to that for the 'solenoid coil with one yoke'.

In the case of using the 'split coil with two yokes' at 13 K, shown in figures 5(e) and (f), the peak height of $B_z(t)$ is nearly the same as that of $B_{ex}(t)$, which is a common characteristic for the split coil. However, it should be noticed that the intrusion of the magnetic flux was delayed in the case with the yoke, which is in clear contrast to the case without the yoke, as shown in figures 5(c) and (d). The local field, $B_z(t)$, takes a maximum and then becomes flat with increasing time. For $B_{ex} = 1.61$ T, a $B_z = 1.10$ T (1.04 T after the yoke is removed) was achieved. For $B_{ex} = 2.31$ T, B_z decreases and a flux jump was not observed up to $B_{ex} = 2.95$ T.

Figure 6(a) shows the time dependence of the temperature, $T(t)$, after applying pulsed fields at 20 K using the split coil with two yokes. The maximum temperature, T_{max}, as a function of B_{ex} is also shown in the inset. Note that $T(t)$ was measured on the copper holder shown in figure 1(a). $T(t)$ takes a maximum within 2 s for each case and the maximum temperature, T_{max}, increases with increasing B_{ex}, which is independent of the cases with and without yoke. Figure 6(b) shows the $T(t)$ after applying pulsed fields at 20 K using the solenoid coil with one yoke, which was measured on the bulk surface shown in figure 1(b). T_{max}, as a function of B_{ex}, is also shown in the inset. $T(t)$ increases with increasing B_{ex}. The temperature rise was recovered within 30–40 s, which is longer than that for the case using split coil, and the temperature rise seems to be larger than that for the split coil. However, we must be careful not compare the results of figures 6(a) to (b) directly, because the position of the temperature measurement was different and the temperature for the split coil was not measured on the bulk surface.

5. Numerical simulation results and discussion

Figure 7 presents the results of the numerical simulation for a normalized magnetic pulse, $B_{ex}(t)$, using the split coils with and without two yokes and the solenoid coil with one yoke. An imaginary $B_{ex}(t)$ curve for the solenoid coil without the yoke is also shown, which corresponds to the current pulse shown in equation (2), and takes a maximum at $\tau = 0.013$ s. For $B_{ex}(t)$ for the solenoid coil with one yoke, the yoke resulted in a moderately slower decay of the magnetic pulse, compared to $B_{ex}(t)$ for the solenoid coil without yoke. On the other hand, $B_{ex}(t)$ takes a maximum at $\tau = 0.018$ s for the split coil without yoke, according to equation (2). A more moderate decrease in the magnetic pulse took place for the split coil with two yokes due to the existence of the yoke. These results can qualitatively reproduce the experimental results shown in figure 4.

Figure 8 shows the results of the numerical simulation of the trapped field, B_z, at 20 K, as a function of the applied pulsed field, B_{ex}, when using each magnetizing coil. The experimental results in figure 3(a) are shown again for reference. In all cases, the magnetic flux intruded and was trapped in the center of the bulk surface, which took a

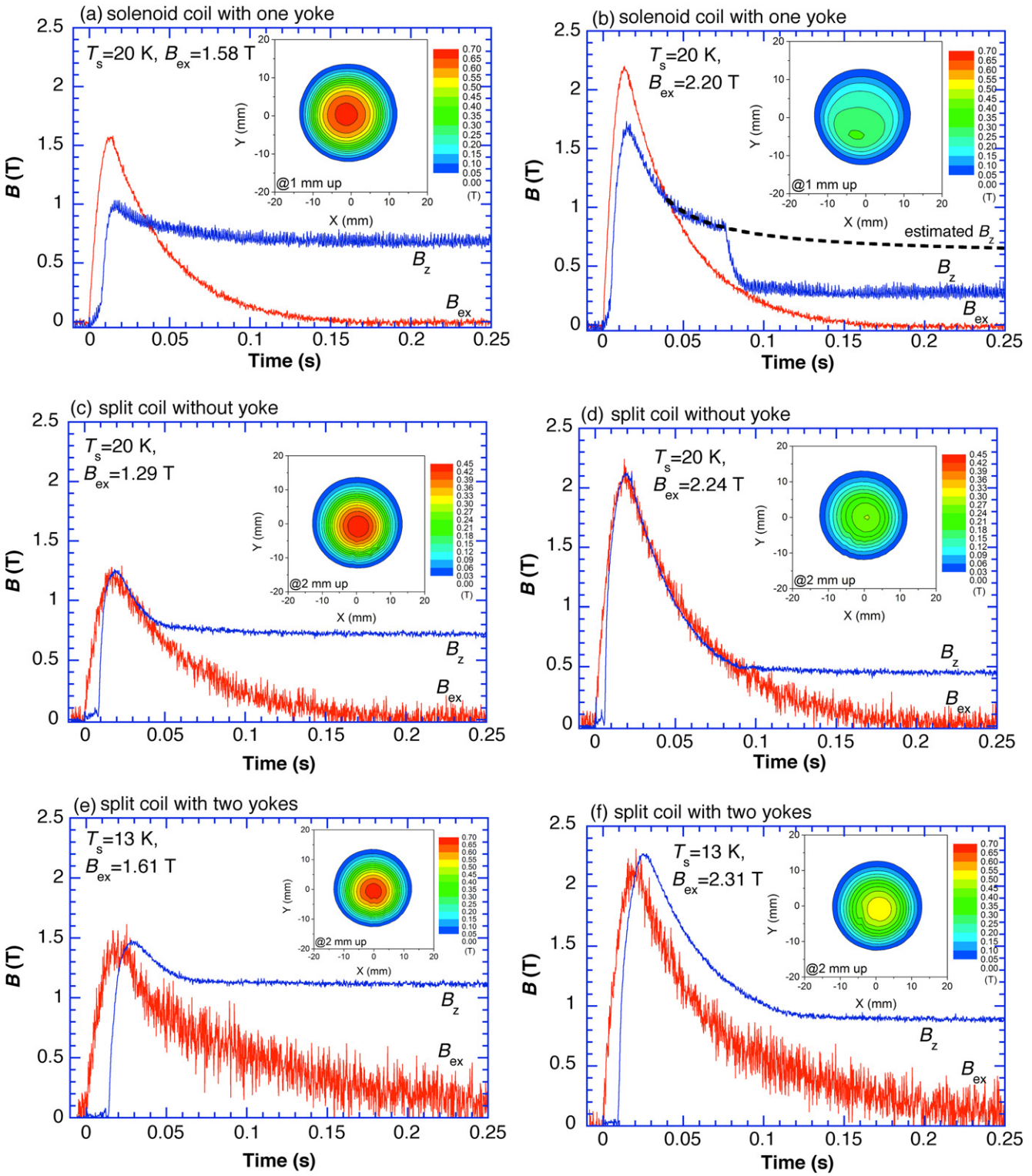

Figure 5. Time dependence of local field, $B_z(t)$, at the center of the bulk surface and the applied field, $B_{ex}(t)$, using the 'solenoid coil with one yoke' at $T_s = 20$ K and (a) $B_{ex} = 1.58$ T and (b) $B_{ex} = 2.20$ T; using the 'split coil without yoke' at $T_s = 20$ K and (c) $B_{ex} = 1.29$ T and (d) $B_{ex} = 2.24$ T, and using the 'split coil with two yokes' at $T_s = 13$ K and (e) $B_{ex} = 1.61$ T and (f) $B_{ex} = 2.31$ T. The 2D trapped field profiles, B_z (1 mm), measured 1 mm above the bulk surface are shown in the insets of (a) and (b), and B_z (2 mm), measured 2 mm above the bulk surface are shown in the insets from (c) to (f).

maximum and then decreased with increasing B_{ex}. The maximum B_z for the 'split coil with two yokes' is larger than those for the 'split coil without yoke' and for the 'solenoid coil with one yoke'. These results of the simulation reproduce the experimental ones well. However, the actual B_{ex} values, at which the magnetic flux starts to intrude into the center of the bulk surface, are not consistent with those obtained by the experiments. These results may result from differences

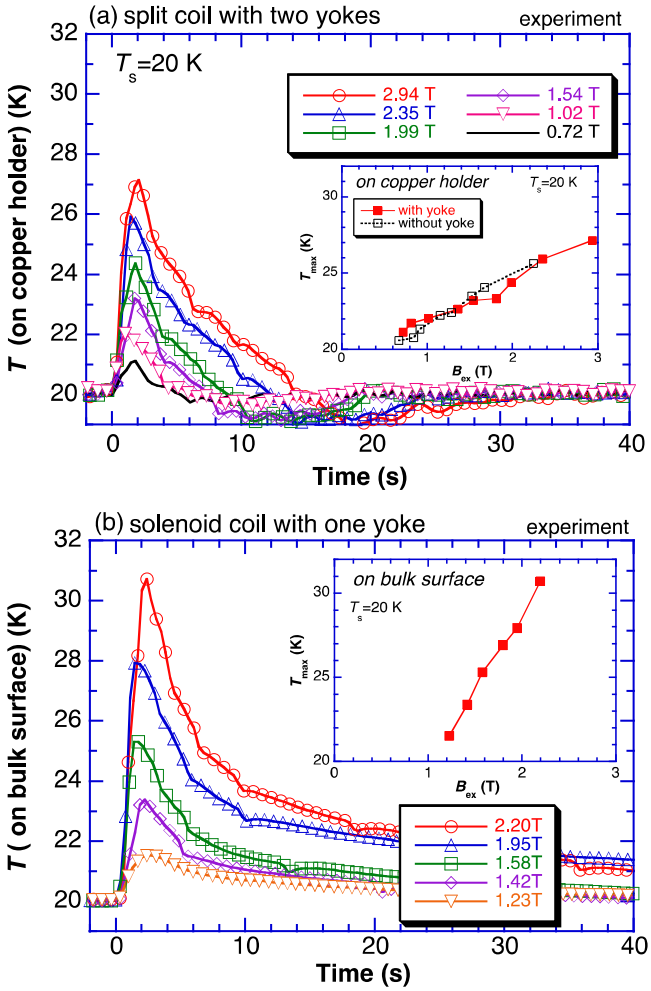

Figure 6. Time dependence of temperature, $T(t)$, after applying the pulsed field using (a) split coil with two yokes and (b) solenoid coil with one yoke at $T_s = 20$ K for various applied pulsed fields, B_{ex}. The maximum temperature, T_{max}, as a function of applied field B_{ex}, is also shown in the insets. $T(t)$ was measured on the copper holder in (a) and on the bulk surface in (b).

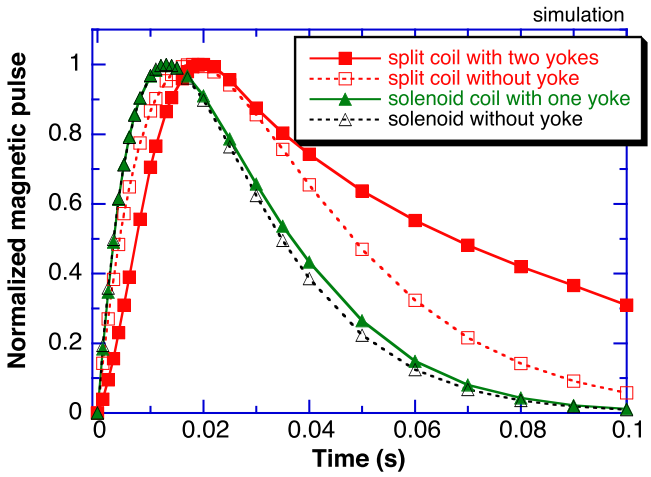

Figure 7. Time evolution of the normalized applied pulsed fields, $B_{ex}(t)$, for the split coil (with and without yokes) and the solenoid coil (with and without yoke), obtained by numerical simulation.

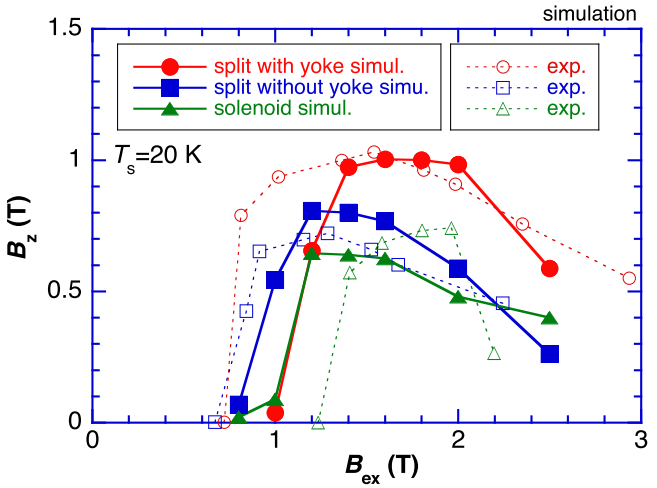

Figure 8. The results of the simulation of trapped field, B_z, versus applied field, B_{ex}, at 20 K using the split coils with/without two yokes and the solenoid coil with one yoke.

between the experimental conditions and the ideal numerical simulation. However, on the whole, the results of the numerical simulation can qualitatively reproduce the experimental results for the trapped field, B_z.

Figures 9(a) and (b) present the time dependences of the local field, $B_z(t)$, at $T_s = 20$ K and $B_{ex} = 1.6$ T for the split coils with/without two yokes and the solenoid coil with one yoke, respectively. The applied field, $B_{ex}(t)$, is also shown for each case. For the split coil with yoke shown in figure 9(a), the magnetic field, $B_z(t)$, takes a maximum with a slight time delay and with nearly the same amplitude of the B_{ex} peak, gradually decreases and then takes a constant B_z value at $t > 0.1$ s. For the split coil without yoke, the time delay at the peak is smaller than that for the split coil with two yokes and the B_z value is smaller. For the solenoid coil with one yoke shown in figure 9(b), the peak height of $B_z(t)$ is smaller than that of $B_{ex}(t)$ and the peak occurred at nearly the same time. These results reproduce the experimental ones shown in figure 5 well.

Figures 10(a) and (b) show the numerical simulation results of the time dependence of the temperature, $T(t)$, at $T_s = 20$ K and $B_{ex} = 1.6$ T for the split coil with two yokes and the solenoid coil with one yoke, respectively. The $T(t)$ values are extracted at three positions; center $(x, z) = (0, 0)$, middle $(x, z) = (5\text{ mm}, 0)$ and side $(x, z) = (10\text{ mm}, 0)$ in the bulk. The maximum $T(t)$ increased from the bulk periphery for both cases, took a maximum around the peak of the applied pulse and then decreased from the bulk periphery. The temperature recovery to the initial temperature, $T_s = 20$ K, for the split coil is faster than that for the solenoid coil with one yoke, which results from the difference of the surface area attached to the holder and the difference in its thermal conductivity. The faster $T(t)$ peak and the prompt $T(t)$ recovery within 1 s results from the small specific heat, C, and large thermal conductivity, κ, of the present MgB_2 bulk at $T_s = 20$ K, which is in clear contrast with the similar numerical simulation results for REBaCuO at $T_s = 40$ K [22], in

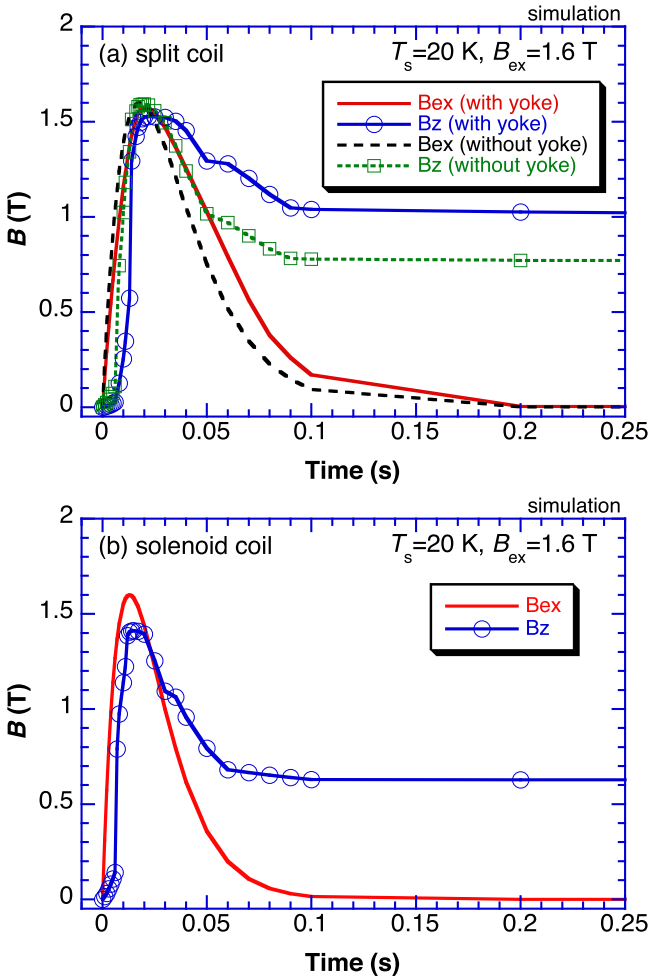

Figure 9. Numerical simulation results of the time dependence of the local field, $B_z(t)$, and applied pulsed field, $B_{ex}(t)$, at the center of the bulk at $T_s = 20$ K and $B_{ex} = 1.6$ T for (a) split coils with/without yokes and (b) the solenoid coil with yoke.

which $T(t)$ takes a maximum at around 1 s at the center of the bulk surface due to the large C value of 132 J kg^{-1} K^{-1} and relatively small κ value along the c-axis of 4 W mK^{-1}. On the other hand, the C and κ values of the MgB_2 bulk used in the simulation are 2.9 J kg^{-1} K^{-1} and 20 W mK^{-1}, respectively [14]. These results imply that the heat generation and propagation in the present MgB_2 bulk are quite different to those in the GdBaCuO bulk.

Figure 10(c) shows the numerical simulation results of the maximum temperature, T_{max}, during the PFM process at $T_s = 20$ K, as a function of the applied pulsed field, B_{ex}, for the cases using split coil with and without yoke and the solenoid coil with yoke. In all cases, T_{max} increases with increasing B_{ex}. The T_{max} versus B_{ex} relation seems to be independent of the type of the magnetizing coil and whether or not the yoke is present. These results suggest that the experimental results of B_z shown in figure 3 cannot be explained by the difference of the temperature rise directly. The kink behavior at around $B_{ex} = 1$ T may be related to the abrupt flux intrusion to the bulk center.

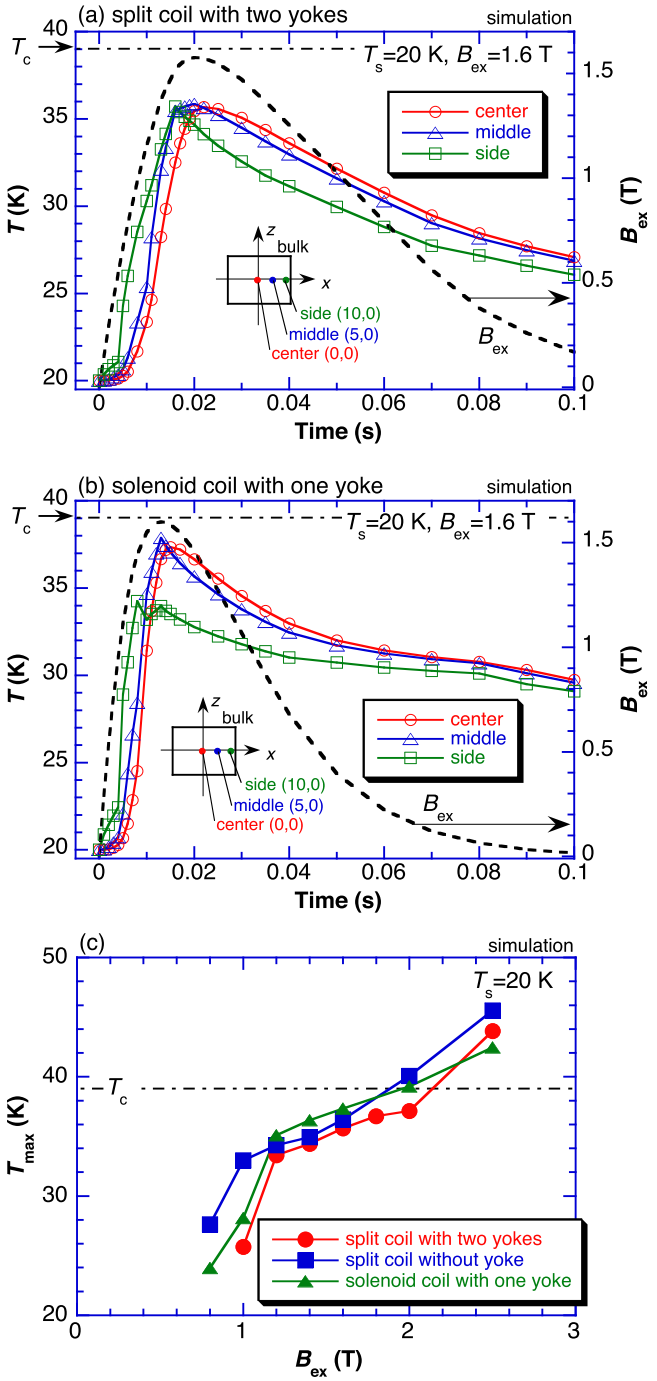

Figure 10. Numerical simulation results of the maximum temperature, T_{max}, during PFM at $T_s = 20$ K, as a function of the applied pulsed field, B_{ex}, for the cases using the split coils with/without two yokes and the solenoid coil with one yoke.

Finally, let us consider the effect of the soft iron yoke on the enhancement of the trapped field, B_z. Figure 11 shows images of the magnetic flux vector distribution at $t = 0.3$ s after the magnetic pulse application of $B_{ex} = 1.6$ T at $T_s = 20$ K using the split coils with and without the soft iron yoke. For the split coil with yoke shown in figure 11(a), the induced magnetic flux in the bulk was pulled along the yoke (z-direction) during the PFM process, and, as a result, the final

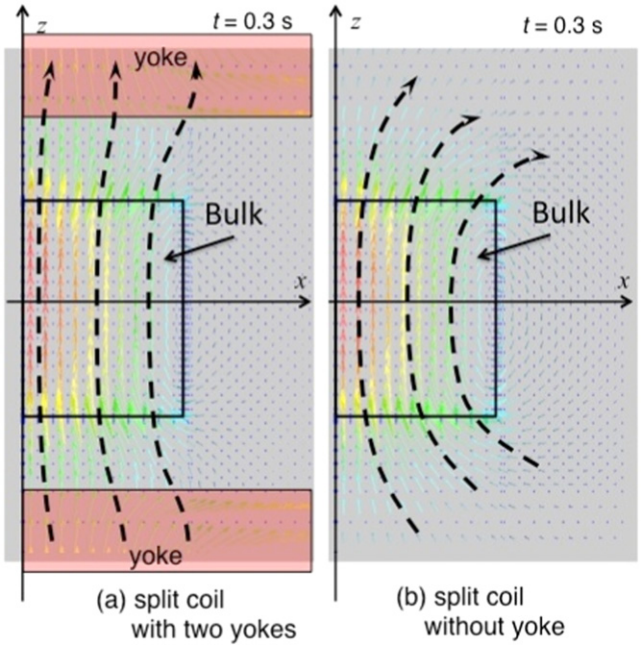

Figure 11. Images of the magnetic flux vector distribution around the bulk after applying a magnetic pulse of $B_{ex} = 1.6$ T at $T_s = 20$ K using (a) split coil with two yokes and (b) split coil without yoke.

B_z value was enhanced. The trapped flux distribution, aligned to the z-direction, remained, even if the yoke was removed after the PFM procedure. On the other hand, for the split coil without yoke shown in figure 11(b), the flux lines curved out of the bulk, and the component in the z-direction, i.e., the B_z value, became relatively smaller. In this way, the soft iron yokes on both bulk surfaces is significantly effective to enhance the B_z value and the subsequent total trapped flux Φ_z.

6. Conclusion

We have investigated the PFM for a high-J_c MgB_2 bulk using a split-type coil and compared the results to those using a solenoid-type coil. We have also studied the effect of the soft iron yoke inserted in the bores of split-type coil to enhance the trapped field, B_z.

A trapped field of $B_z = 1.1$ T was achieved on the MgB_2 bulk at 13 K without flux jumps by PFM using a split-type coil with soft iron yoke, which is a record-high trapped field by PFM on an MgB_2 bulk to date. Flux jumps, which frequently took place using a solenoid-type coil during PFM, were avoided by using the split-type coil, even for higher applied pulsed fields, B_{ex}. The applied magnetic field, $B_{ex}(t)$, rises up slowly and decreases slowly, compared to that for the solenoid coil with one yoke, which is one of the possible reasons to avoid the flux jumps.

The B_z value was significantly enhanced by the insertion of soft iron yokes in the bores of the split coil, which mainly results from the flux alignment effect of the yoke. The alignment of the trapped magnetic flux in the z-direction was almost maintained, even if the split coil with yoke was removed after the PFM procedure.

The flux dynamics and heat generation/propagation were analyzed during these PFM processes using numerical simulations and these can qualitatively reproduce the experimental results well. The magnetic flux intrudes and then attenuates more slowly in the bulk and tends to be aligned along the z-direction due to the presence of soft iron yoke.

Acknowledgments

This work was supported by Open Partnership Joint Projects of Japan Society for the Promotion of Science (JSPS) Bilateral Joint Research Projects, and JSPS KAKENHI grant number 23560002 and 15K04646. Dr Mark Ainslie would like to acknowledge the support of a Royal Academy of Engineering Research Fellowship and a Royal Society International Exchanges Scheme grant, IE131084.

References

[1] Zou J, Ainslie M D, Fujishiro H, Bhagurkar A G, Naito T, Hari Babu N, Fagnard J-F, Vanderbemden P and Yamamoto A 2015 *Supercond. Sci. Technol.* **28** 075009
[2] Ainslie M D, Fujishiro H, Ujiie T, Zou J, Dennis A R, Shi Y-H and Cardwell D A 2014 *Supercond. Sci. Technol.* **27** 065008
[3] Kambara M, Babu N H, Sadki E S, Cooper J R, Minami H, Cardwell D A, Campbell A M and Inoue I H 2001 *Supercond. Sci. Technol.* **14** L5
[4] Durrell J H, Dancer C E J, Dennis A, Shi Y, Xu Z, Campbell A M, Hari N, Todd R I, Grovenor C R M and Cardwell D A 2012 *Supercond. Sci. Technol.* **25** 112002
[5] Yamamoto A, Ishihara A, Tomita M and Kishio K 2014 *Appl. Phys. Lett.* **105** 032601
[6] Naito T, Yoshida T and Fujishiro H 2015 *Supercond. Sci. Technol.* **28** 095009
[7] Fuchs G, Häßler W, Nenkov K, Scheiter J, Perner O, Handstein A, Kanai T, Schultz L and Holzapfel B 2013 *Supercond. Sci. Technol.* **26** 122002
[8] Yanagi Y, Itoh Y, Yoshikawa M, Oka T, Hosokawa T, Ishihara H, Ikuta H and Mizutani U 2000 *Advances in Superconductivity* vol 12 (Tokyo: Springer) p 470
[9] Sander M, Sutter U, Koch R and Klaser M 2000 *Supercond. Sci. Technol.* **13** 841
[10] Fujishiro H, Tateiwa T, Fujiwara A, Oka T and Hayashi H 2006 *Physica* C **445–448** 334
[11] Fujishiro H, Tamura T, Arayashiki T, Oyama M, Sasaki T, Naito T, Giunchi G and Albisetti A F 2012 *Japan. J. Appl. Phys.* **51** 103005
[12] Fujishiro H, Ujiie T, Naito T, Albisetti A F and Giunchi G 2014 *J. Phys.: Conf. Ser.* **507** 032016
[13] Fujishiro H, Ujiie T, Mochizuki H, Yoshida T and Naito T 2015 *IEEE Trans. Appl. Supercond.* **25** 6800104
[14] Fujishiro H, Mochizuki H, Naito T, Ainslie M D and Giunchi G 2016 *Supercond. Sci. Technol.* **29** 034006
[15] Ida T *et al* 2004 *Physica* C **412–414** 638
[16] Fujishiro H, Naito T and Oyama M 2011 *Supercond. Sci. Technol.* **24** 075015

[17] Fujishiro H, Fujiwara A, Tateiwa T, Oka T and Hayashi H 2006 *IEEE Trans. Appl. Supercond.* **16** 1080
[18] Hiyama T, Fujishiro H, Tateiwa T, Naito T, Hayashi H and Tone K 2008 *Physica* C **468** 1469
[19] Ikuta H, Ishihara H, Yanagi Y, Itoh Y and Mizutani U 2002 *Supercond. Sci. Technol.* **15** 606
[20] Gony B, Berger K, Douine B, Koblischka R and Leveque J 2015 *IEEE Trans. Appl. Supercond.* **25** 8801005
[21] Ainslie M D and Fujishiro H 2015 *Supercond. Sci. Technol.* **28** 053002
[22] Fujishiro H and Naito T 2011 *Supercond. Sci. Technol.* **23** 105021